# Supplementary Materials: Synthesis, Crystal Structure, Electrochemistry and Electro-Catalytic Properties of the Manganese-Containing Polyoxotungstate, $[(Mn(H_2O)_3)_2(H_2W_{12}O_{42})]^{6-}$

**Anne-Lucie Teillout, Pedro de Oliveira, Jérôme Marrot, Robertha C. Howell, Neus Vilà, Alain Walcarius and Israël M. Mbomekallé ***

**S1.** Electrochemistry

**S1.1.** Comparison between $[(Mn(H_2O)_3)_2(H_2W_{12}O_{42})]_2^{6-}$ and its Parent's Counterparts $[H_2W_{12}O_{40}]^{6-}$ and $[H_2W_{12}O_{42}]^{10-}$

**S1.2.** Determination of the Diffusion Coefficient

**S1.3.** pH Influence

**S1.4.** Electro-Catalytic Reduction of Nitrite and Dioxygen by **1** on GCE

**S1.5.** $Mn^{2+}$ Redox Steps in **1**, $[Mn^{II}(H_2O)SiW_{11}O_{39}]^{6-}$ and $[Mn^{II}_4(H_2O)_2(SiW_9O_{34})_2]^{12-}$

**S1.6.** Influence of the Electrolyte at Different pH Values

**S2.** XPS Spectra

**S3.** UV-Visible Spectra

**S4.** FT-IR Spectra

**S5.** Thermogravimetric Analysis

## S1. Electrochemistry

### S1.1. Comparison between $[(Mn(H_2O)_3)_2(H_2W_{12}O_{42})]^{6-}$ and its parent's counterparts $[H_2W_{12}O_{40}]^{6-}$ and $[H_2W_{12}O_{42}]^{10-}$

The medium 0.5M $Li_2SO_4$ + $H_2SO_4$ / pH 3 was selected for a direct comparison between the electrochemical behaviors of the three parent compounds. In this medium, the reduction of $[H_2W_{12}O_{42}]^{10-}$ on a glassy carbon electrode (GCE) is irreversible and occurs at very low potential (−0.88 V vs. SCE). This is not surprising given its formal anionic charge, −10. Polymerization of this polyanion by complexation of two $Mn^{2+}$ between two $[H_2W_{12}O_{42}]^{10-}$ moieties induces several physical and chemical changes that affected electrochemical properties of the new compound, the monomer $[(Mn(H_2O)_3)_2(H_2W_{12}O_{42})]^{6-}$ (**1**). Reduction of **1** becomes easier with three successive one-electron processes located between −0.3 and −0.8 V. For better visualization, Figures S2 below show (A) superimposed CVs of $[H_2W_{12}O_{42}]^{10-}$ and $[H_2W_{12}O_{40}]^{6-}$ and (B) superimposed CVs of $[H_2W_{12}O_{40}]^{6-}$ and **1**. Electrochemical properties of $[H_2W_{12}O_{42}]^{10-}$ are not within the scope of this paper and those of $[H_2W_{12}O_{40}]^{6-}$ have been largely discussed in several studies.

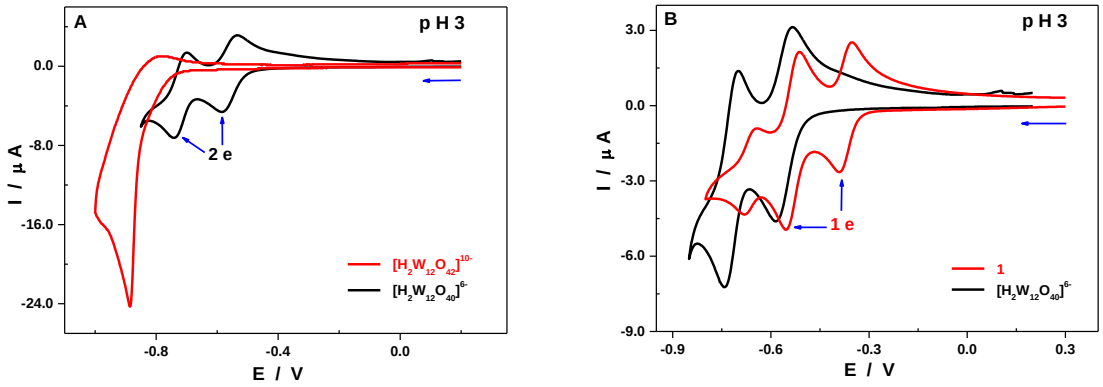


**Figure S1.** CVs of **1**, $[H_2W_{12}O_{40}]^{6-}$ and $[H_2W_{12}O_{42}]^{10-}$ in 0.5M $Li_2SO_4$ + $H_2SO_4$ / pH 3. Polyoxometalate concentration: 0.5 mM; scan rate: 10 $mV \cdot s^{-1}$; working electrode: glassy carbon; reference electrode: SCE.
(A) Comparison between CV of $[H_2W_{12}O_{42}]^{10-}$ (red line) and CV of $[H_2W_{12}O_{40}]^{6-}$ (black line).
(B) Comparison between CV of **1** (red line) and CV of $[H_2W_{12}O_{40}]^{6-}$ (black line).

### S1.2. Determination of the Diffusion Coefficient

In order to demonstrate that the compound **1** exists as the $[(Mn(H_2O)_3)_2(H_2W_{12}O_{42})]^{6-}$ monomer in solution, its diffusion coefficient, **D**, was determined and compared to that of metatungstate, $[H_2W_{12}O_{40}]^{6-}$, a Keggin-type species carrying the same charge as **1**. The CVs of the two compounds were recorded in the same experimental conditions in 0.5M $Li_2SO_4$ + $H_2SO_4$, pH 3.0, at scan rates ranging from 10 to 100 $mV \cdot s^{-1}$. The square of the reduction peak current, $(I_{pc})^2$, of the first wave was plotted as a function of the scan rate. The slope of the plot $(I_{pc})^2 = f(v)$ allows to estimate the value of the diffusion coefficient of the studied species, according to the Randles - Sevcik equation: $I_{pc} = 2.69.10^5 \times n^{3/2} \times A \times D^{1/2} \times v^{1/2} \times C$ (see Figure SI-1).

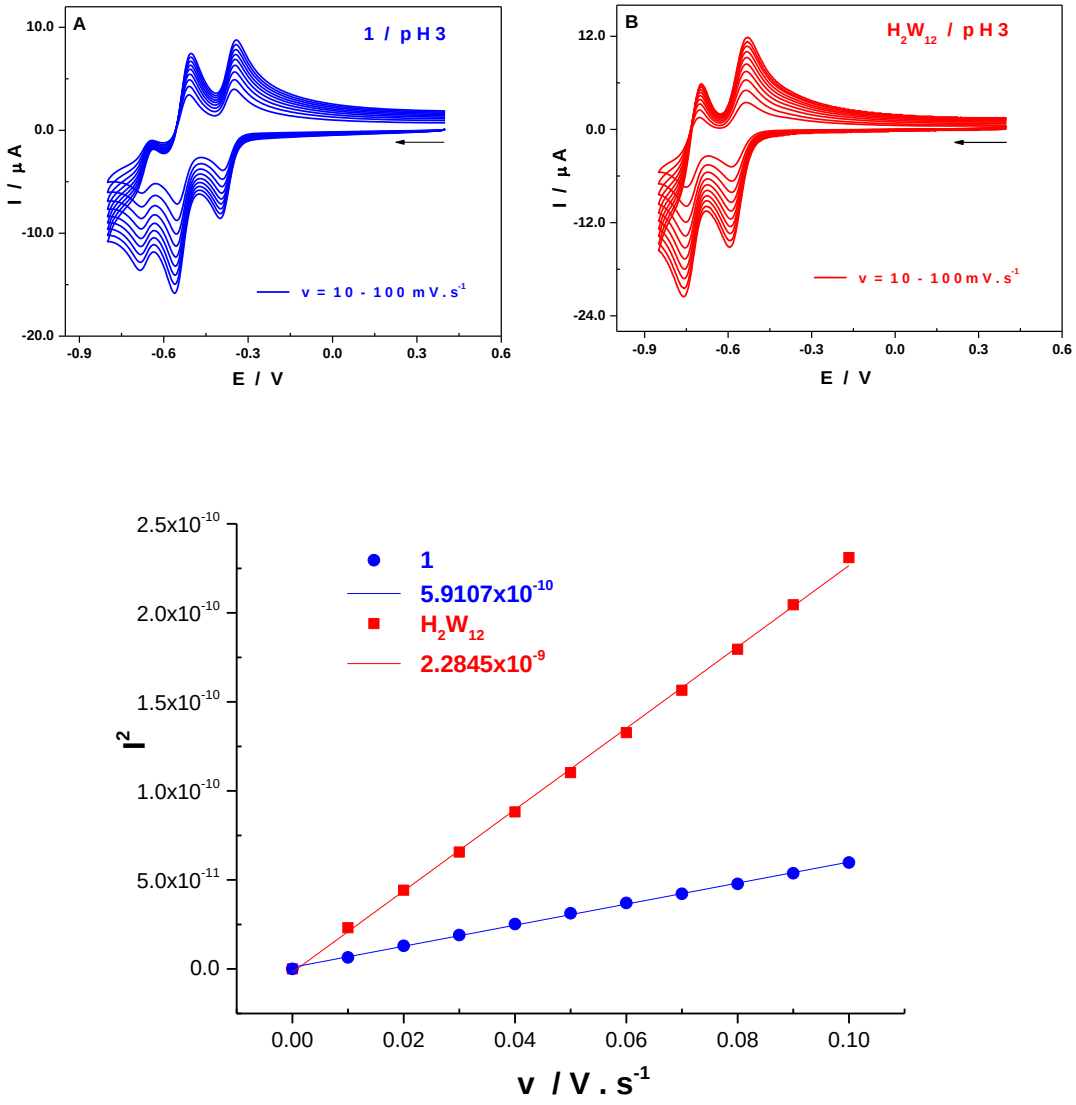


**Figure S2.** CVs of **1** (A) and $[H_2W_{12}O_{40}]^{6-}$ (B) in 0.5M $Li_2SO_4$ + $H_2SO_4$ / pH 3. Polyoxometalate concentration: 0.5 mM; scan rate varying from 10 to 100 $mV \cdot s^{-1}$ ; working electrode: glassy carbon; reference electrode: SCE.

(C) Evolution of the square of the reduction peak current of the first wave as a function of the scan rate, $(I_{pc})^2 = f(v)$, for 1 (blue) and for $[H_2W_{12}O_{40}]^{6-}$ (red).

**Table S1.**

| **1** | | **$[H_2W_{12}O_{40}]^{6-}$** | |
|---|---|---|---|
| v | $(I_{pc})^2$ | v | $(I_{pc})^2$ |
| 0 | 0 | 0 | 0 |
| 0.01 | 6.5025E-12 | 0.01 | 2.3136E-11 |
| 0.02 | 1.3032E-11 | 0.02 | 4.4223E-11 |
| 0.03 | 1.901E-11 | 0.03 | 6.561E-11 |
| 0.04 | 2.52E-11 | 0.04 | 8.8172E-11 |
| 0.05 | 3.1248E-11 | 0.05 | 1.1025E-10 |
| 0.06 | 3.7088E-11 | 0.06 | 1.3271E-10 |
| 0.07 | 4.225E-11 | 0.07 | 1.565E-10 |
| 0.08 | 4.7748E-11 | 0.08 | 1.7956E-10 |
| 0.09 | 5.3729E-11 | 0.09 | 2.0449E-10 |
| 0.1 | 5.9753E-11 | 0.1 | 2.3104E-10 |

Randles - Sevcik equation : $I_{pc} = 2.69.10^5 \times n^{3/2} \times A \times D^{1/2} \times v^{1/2} \times C$
$I_{pc}$ : cathodic peak current (A)
n : number of electrons exchanged per molecule
A : electrode surface ($cm^2$) = 0.0707 $cm^2$
D : diffusion coefficient ($cm^2 \cdot s^{-1}$)
v : scan rate ($V \cdot s^{-1}$)
C : concentration ($mol \cdot cm^{-3}$)

**[1] = $5.31\times10^{-4}$ mol·$L^{-1}$ = $5.31\times10^{-7}$ mol·$cm^{-3}$**

From the plot $(I_{pc})^2 = f(v)$ → $(I_{pc})^2 = (2.69\times10^5)^2 \times 1^3 \times (0.0707)^2 \times D \times v \times (5.31\times10^{-7})^2$
→ $(I_{pc})^2 = 1.02\times10^{-4}\ D \times v$
→ $1.02\times10^{-4} \times D$ being the slope of the straight line $(I_{pc})^2 = f(v)$.

→ $5.9107\times10^{-10} = 1.02\times10^{-4} \times D$
→ $D = 5.9107\times10^{-10}/1.02\times10^{-4}$
→ **$D = 5.78\times10^{-6}$ $cm^2 \cdot s^{-1}$**

**[$H_2W_{12}$] = $6.53\times10^{-4}$ mol·$L^{-3}$ = $6.53\times10^{-7}$ mol·$cm^{-3}$**

From the plot $(I_{pc})^2 = f(v)$ → $(I_{pc})^2 = (2.69\times10^5)^2 \times 2^3 \times (0.0707)^2 \times D \times v \times (6.53\times10^{-7})^2$
→ $(I_{pc})^2 = 1.23\times10^{-3} \times D \times v$
→ $1.23\times10^{-3} \times D$ being the slope of the straight line $(I_{pc})^2 = f(v)$.

→ $2.2845\times10^{-9} = 1.23\times10^{-3} \times D$
→ $D = 2.2845\times10^{-9}/1.23\times10^{-3}$
→ **$D = 1.86\times10^{-6}$ $cm^2 \cdot s^{-1}$**

The diffusion coefficients of the two compounds, $[(Mn(H_2O)_3)_2(H_2W_{12}O_{42})]_2^{6-}$ and $[H_2W_{12}O_{40}]^{6-}$, are of the same order of magnitude, a clear indication that **1** exists in solution as the monomer having the chemical formula previously presented.

## S1.3. pH Influence

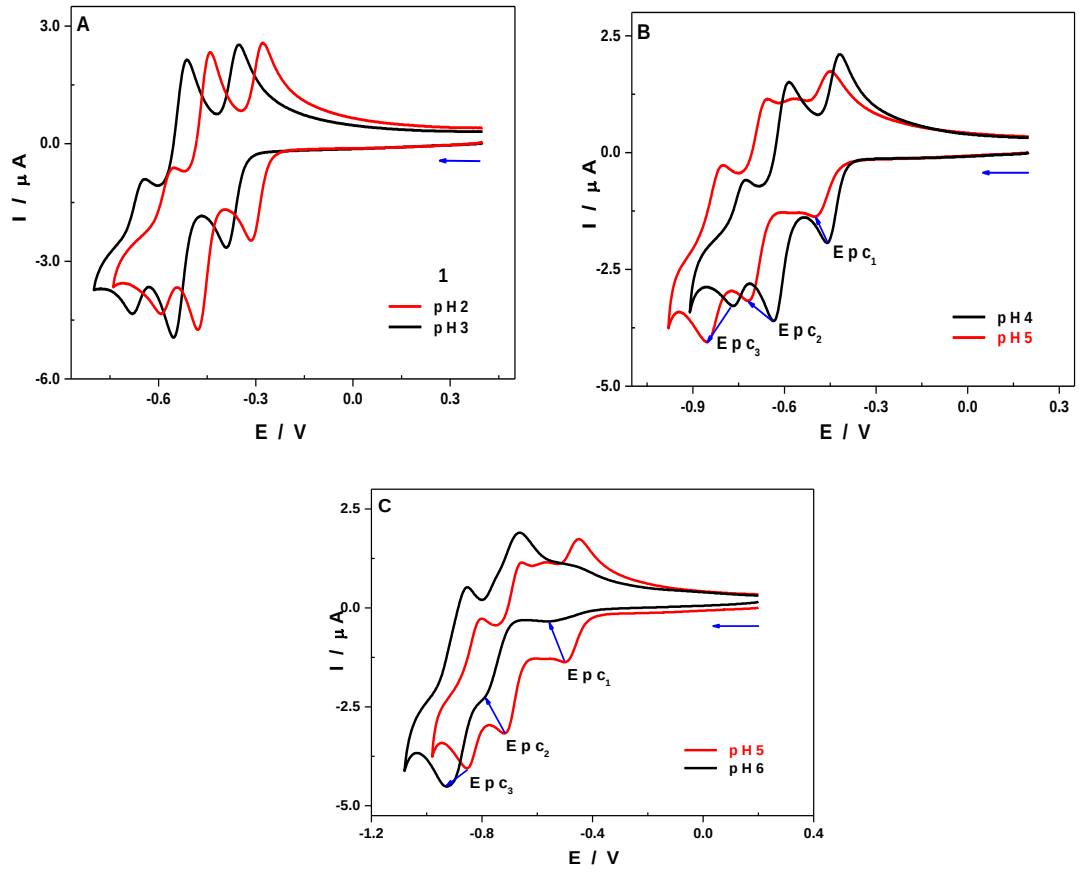


**Figure S3.** CVs of **1** at different pH values**;** POM concentration: 0.5 mM. Scan rate: 10 mV $s^{-1}$; working electrode: glassy carbon; reference electrode: SCE.
(A) pH 2 (red line) and pH 3 (black line);
(B) pH 4 (black line) and pH 5 (red line);
(C) pH 5 (red line) and pH 6 (black line).

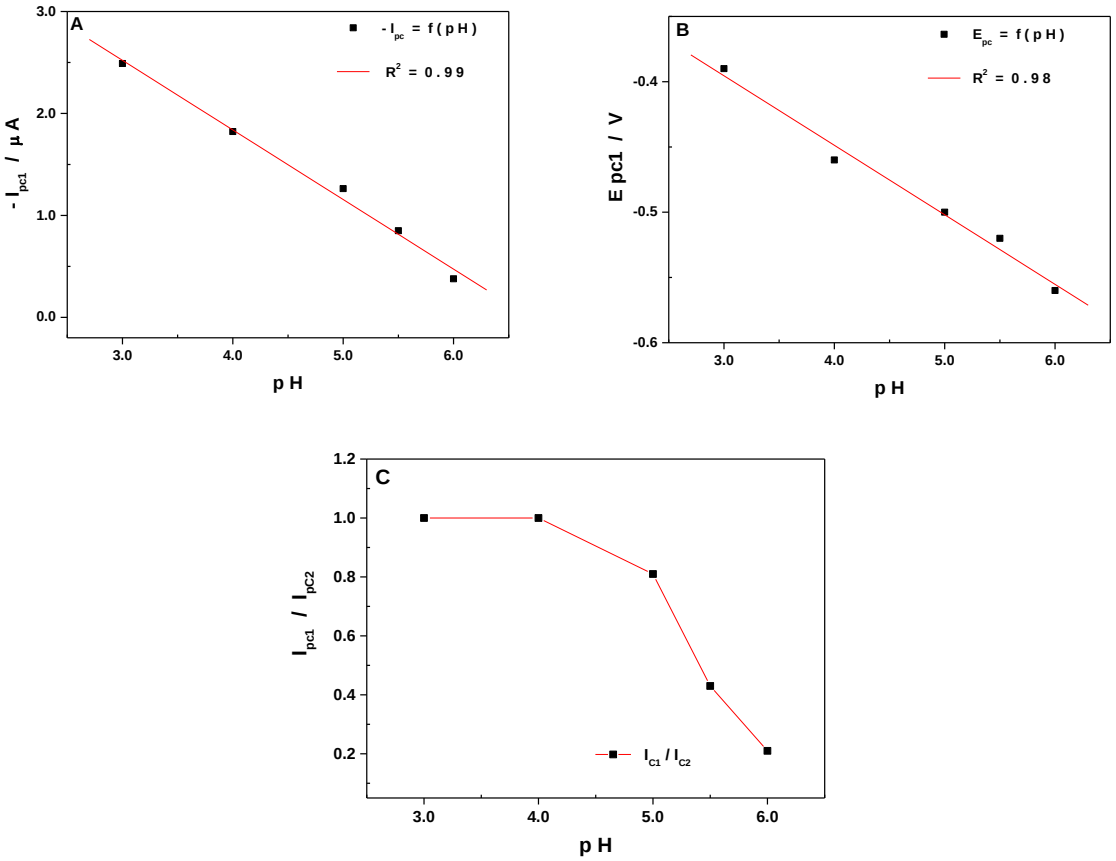


**Figure S4.** (A) Variation of cathodic peak current intensity, $Ipc_1$, for the first wave, as a function of the pH. (B) Variation of the reduction peak potential, $Epc_1$, for the first wave, as a function of the pH. (C) $I_{PC1}/I_{PC2}$ as a function of the pH. CVs are recorded at scan rate of 10 mV $s^{-1}$; working electrode: glassy carbon; reference electrode: SCE.

## S1.4. Electro-Catalytic Reduction of Nitrite and Dioxygen by 1 on GCE

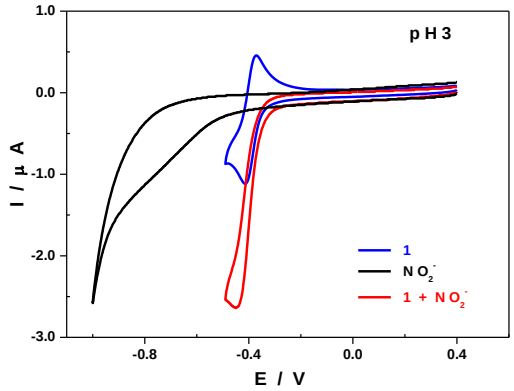


**Figure S5.** CV of **1** only (blue line, concentration: 0.5 mM), in the presence of 40 equivalents of $NO_2^-$ and CV of $NO_2^-$ only (concentration: 2 mM). Electrolyte: 0.5M $Li_2SO_4$ + $H_2SO_4$ / pH 3; scan rate: 10 mV $s^{-1}$; working electrode: glassy carbon; reference electrode: SCE.

The formation of manganese oxides film at the working electrode, actually seems to have a positive effect on the electro-catalytic reduction of $O_2$. In fact, when the potential is scanned initially in the positive direction up to +1.0 V vs. SCE, the electro-catalytic wave anodically shifts about 100 mV when compared to the scan started in the negative direction.

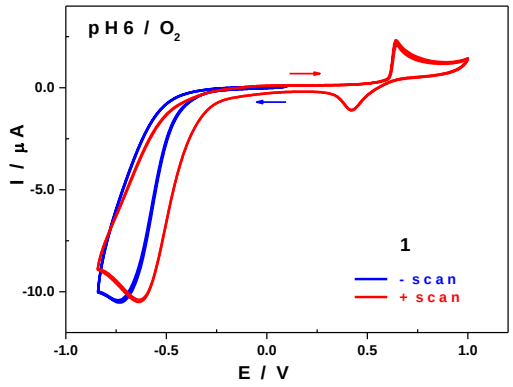


**Figure S6.** Two sets of 2 successive CVs recorded in 1M $CH_3COOLi$ + $CH_3COOH$ / pH. Polyoxometalate concentration 0.5 mM; scan rate 10 mV $s^{-1}$; working electrode: glassy carbon; reference electrode: SCE. Curves in blue: The scan is initially done in the negative potential direction (from +0.1 V to - 0.84 V). The peak potential of $O_2$ electro-catalytic wave is observed at −0.72 V vs. SCE, with an onset estimated at around −0.36 V. Curves in red: The scan is initially done in the positive potential direction (from 0.1 up to +1.0 V) then in the negative potential direction (down to −0.84 V). The peak potential of the $O_2$ electro-catalytic wave is observed at −0.63 V vs. SCE, with an onset estimated at around −0.25 V.

## S1.5. $Mn^{2+}$ redox steps in 1, $[Mn^{II}(H_2O)SiW_{11}O_{39}]^{6-}$ and $[Mn^{II}_4(H_2O)_2(SiW_9O_{34})_2]^{12-}$ [1]

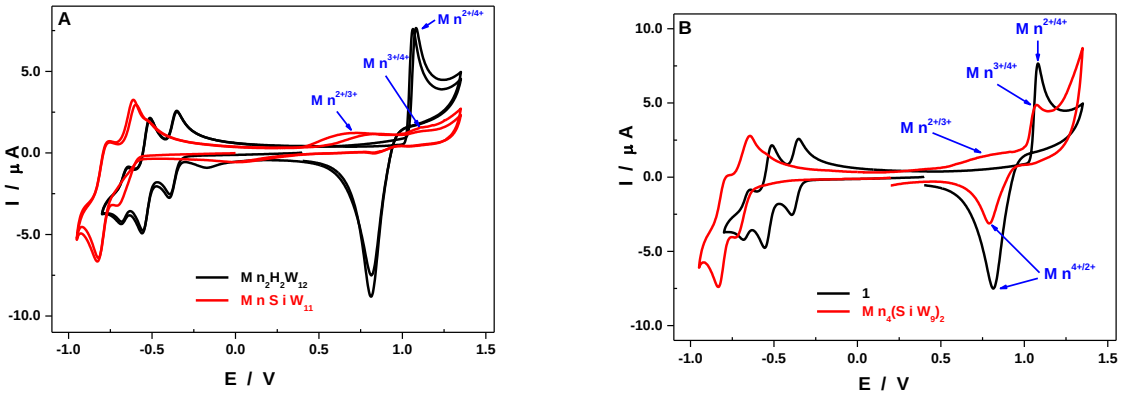


**Figure S7.** CVs obtained in 0.5M $Li_2SO_4$ + $H_2SO_4$ / pH 3; POM concentration 0.5 mM; scan rate 10 mV $s^{-1}$; working electrode: glassy carbon; reference electrode: SCE.
(A) **1** (black line) and $[Mn^{II}(H_2O)SiW_{11}O_{39}]^{6-}$ (red line).
(B) **1** (black line) and $[Mn^{II}_4(H_2O)_2(SiW_9O_{34})_2]^{12-}$ (red line).

## S1.6. Influence of the Electrolyte at Different pH Values

As stated in the main text, one can observe in Figure SI-9A below that a cycling down to −0.3 V vs. SCE is still not sufficient for a perfect regeneration of the working electrode surface, i.e. a complete removal of the manganese oxides film deposited on the glassy carbon working electrode during the oxidation step. The presence of acetate anions (see Figure SI-9B), which are better coordinating species than sulphate ions, seems to somewhat prevent the formation this manganese oxides film on the working electrode surface; CVs are almost superimposable over successive cycling.

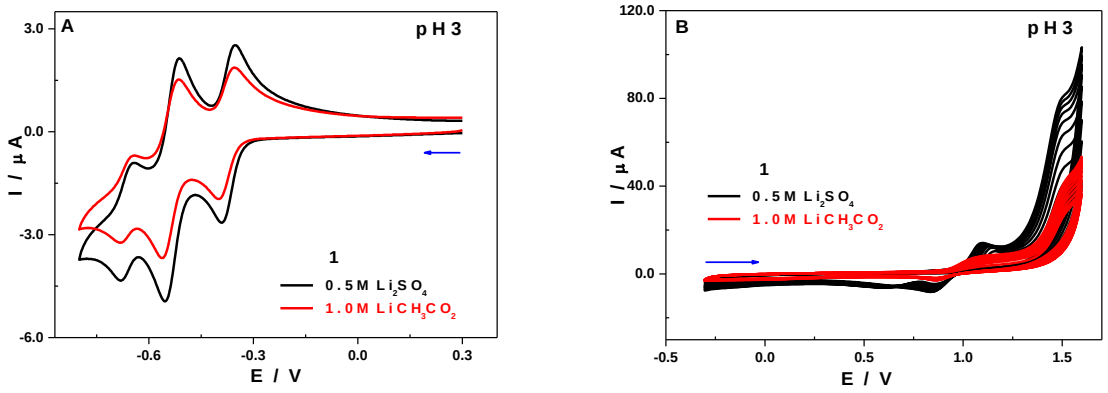


**Figure S8.** CVs of **1** at pH 3 in different media; polyoxometalate concentration: 0.5 mM; scan rate: 10 mV $s^{-1}$; working electrode: glassy carbon; reference electrode: SCE.
(A) Scanning is done in the negative potential direction of from +0.3V to −0.8V in 0.5M $Li_2SO_4$ + $H_2SO_4$ (black line) and in 1M $CH_3COOLi$ + $CH_3COOH$ (red line).
(B) Cycling (10 scans) −0.30V and +1.56V between in 0.5M $Li_2SO_4$ + $H_2SO_4$ (black line) and in 1M $CH_3COOLi$ + $CH_3COOH$ (red line). The scan rate in both cases is 50 mV $s^{-1}$.

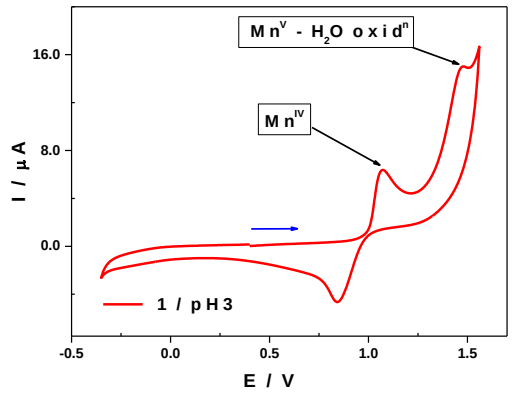


**Figure S9.** CV of **1** in 0.5M $Li_2SO_4$ + $H_2SO_4$ / pH 3. Polyoxometalate concentration: 0.5 mM; scan rate: 10 mV $s^{-1}$; working electrode: glassy carbon; reference electrode: SCE. Potentials were initially scanned up to +1.56 V ($Mn^{5+}$ and $H_2O$ electro-catalytic oxidation) then down to −0.30 V (regeneration of the working electrode surface).

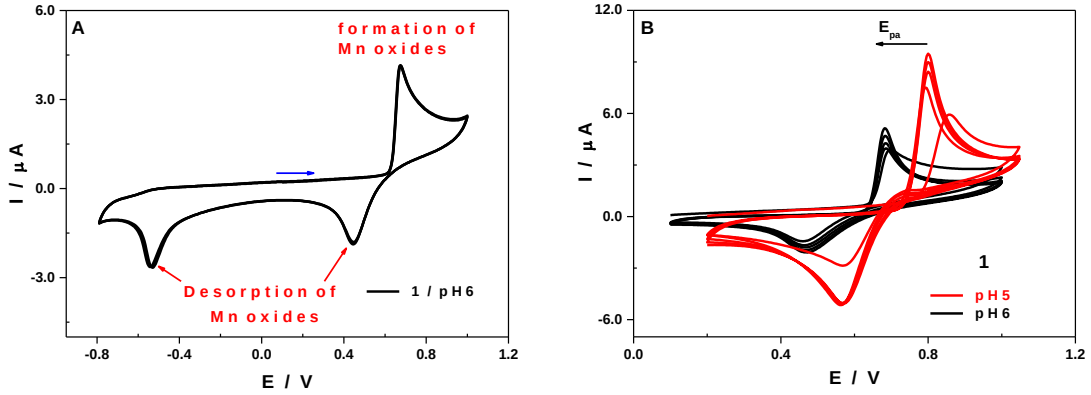


**Figure S10.** (**A**) CVs of **1** in 1M $CH_3COOLi$ + $CH_3COOH$ / pH 6. Cycling (10 cycles) is done between −0.79V and 1.00V.
(**B**) CVs of **1** in 1M $CH_3COOLi$ + $CH_3COOH$, cycling restricted to the $Mn^{2+/4+}$ redox wave: between +0.20V and +1.05V for pH 5 (red line) and between +0.10V and +1.00V for pH 6 (blue line). Polyoxometalate concentration: 0.5 mM; scan rate: 10 mV $s^{-1}$; working electrode: glassy carbon; reference electrode: SCE.
From pH 5 to pH 6 the potential gain is about 150mV {$E_{pa}$(pH5) > $E_{pa}$(pH6)}, but the manganese oxides film grows faster at pH 5 than at pH 6 {$I_{pa}$(pH5) > $I_{pa}$(pH6)}.

## S2. XPS Spectra

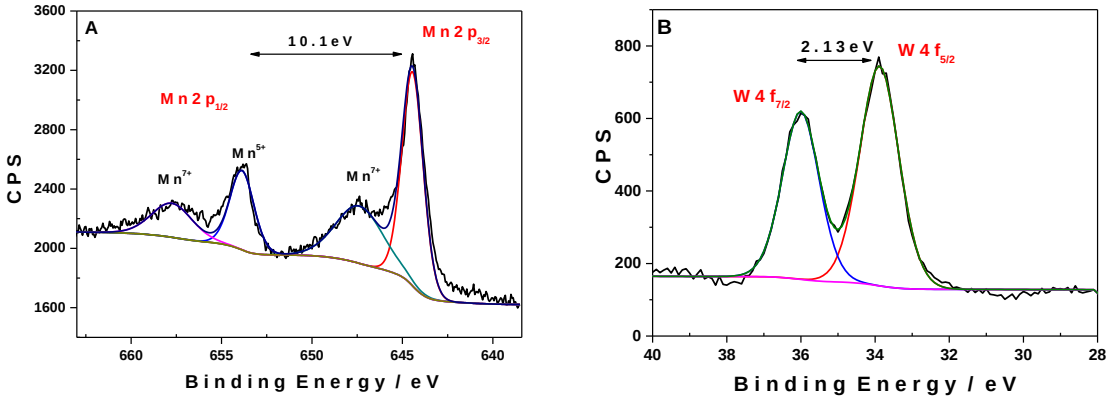


**Figure S11.** XPS survey spectrum for a **1**-modified glassy carbon electrode by induced electrochemical deposition at +1.4 V /SCE in 0.5M $Li_2SO_4$ + $H_2SO_4$ / pH 3. The POM concentration in the solution was 0.5 mM. (**A**) Mn 2p core level spectrum (B) W 4f core level spectrum.

## S3. UV-Visible Spectra

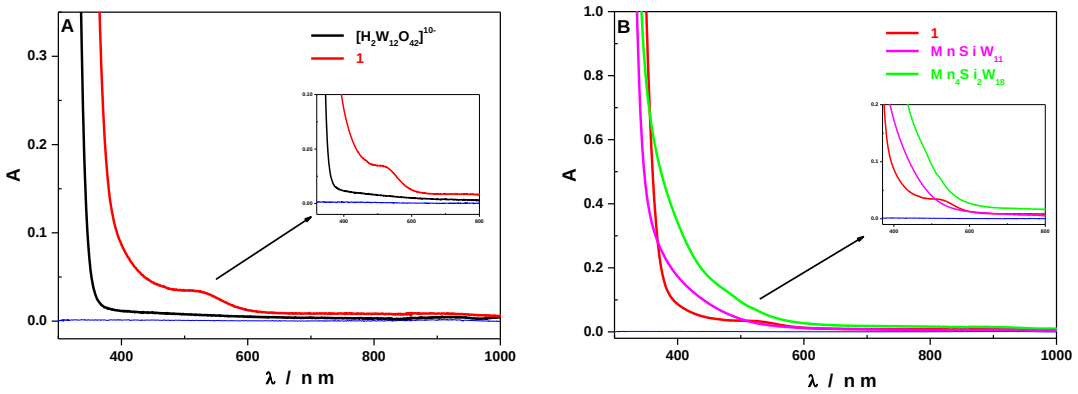


**Figure S12.** UV-visible spectra recorded in 0.5M $Li_2SO_4$ + $H_2SO_4$ / pH 3. (**A**) **1** and $[H_2W_{12}O_{42}]^{10-}$. (**B**) **1** and $[Mn^{II}(H_2O)SiW_{11}O_{39}]^{6-}$ and $[Mn^{II}_4(H_2O)_2(SiW_9O_{34})_2]^{12-}$. POM concentration: 0.5 mM.

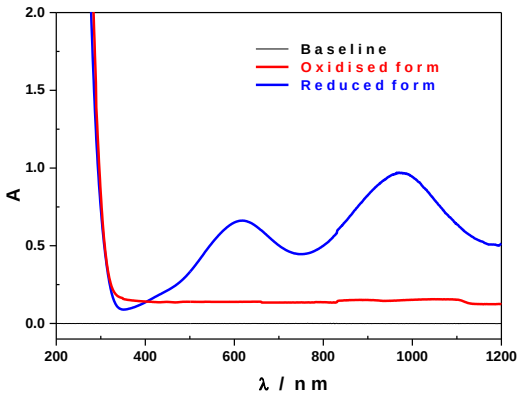


**Figure S13.** UV-visible spectra of **1** recorded in 0.5M $Li_2SO_4$ + $H_2SO_4$ / pH 3; oxidised form (red) and one-electron reduced form (blue). POM concentration: 0.5 mM.

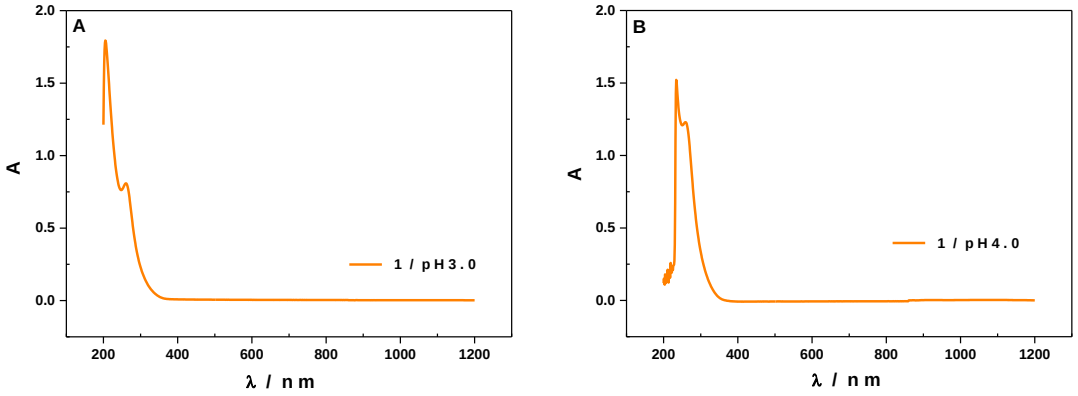


**Figure S14.** UV-visible spectra of 0.15 mM solutions of **1** in (A) 0.5M $Li_2SO_4$ + $H_2SO_4$ / pH 3 and (B) 1M $CH_3COOLi$ + $CH_3COOH$ / pH 4.

## S4. FT-IR Spectra

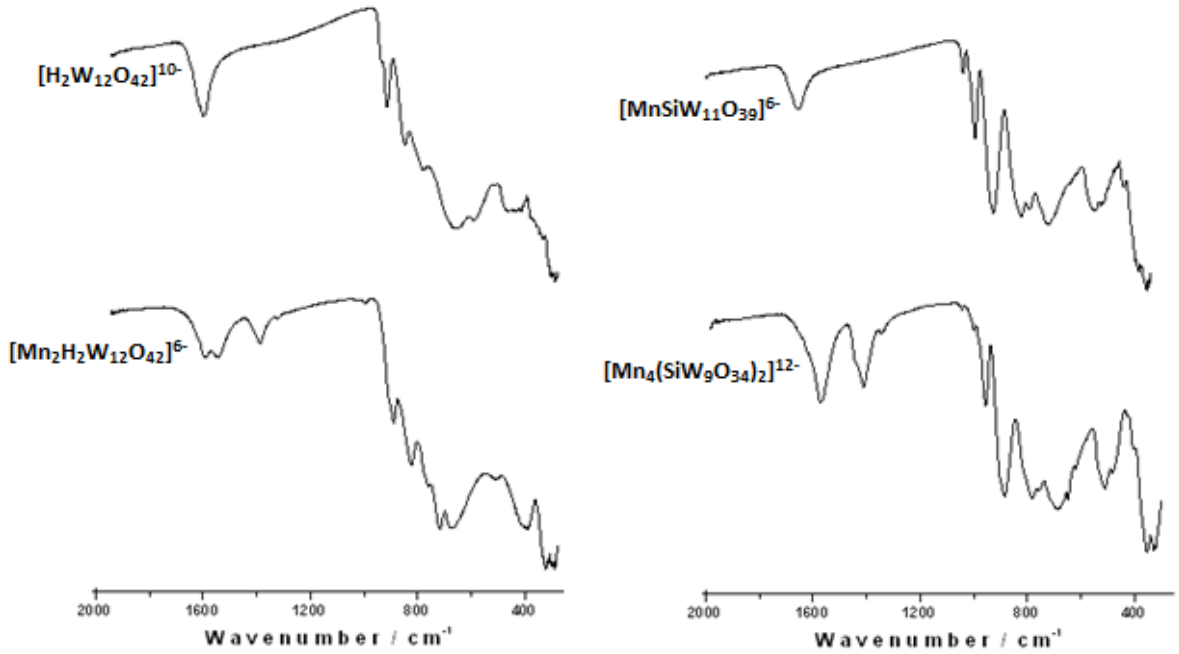


**Figure S15.** FT-IR spectra of **1**, $[H_2W_{12}O_{42}]^{10-}$, $[Mn^{II}(H_2O)SiW_{11}O_{39}]^{6-}$ and $[Mn^{II}{}_4(H_2O)_2(SiW_9O_{34})_2]^{12-}$.

## S5. Thermogravimetric Analysis

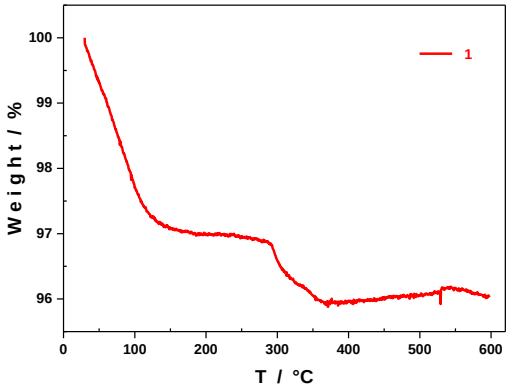


**Figure S16.** Thermogram of **1a** from room temperature to 600 °C.